Supporting Information

Efficient hydrodeoxygenation of guaiacol to phenol over Ru/Ti-SiO_2 catalysts: the significance of defect-rich TiO_x species

Xinchao Wang [a,b,c], Zhuangqing Wang [a,b,c], Leilei Zhou [a,b,c], Yanchun Liu [d], Yinze Yang [a,b,c], Liyan Zhang [a,b,c], Zongling Shang [a,b,c], Hui Li [a,b,c], Tingting Xiao [a,b,c], Chao Zhang* [a,c,e], and Fengyu Zhao* [a,b,c]

[a] State Key Laboratory of Electroanalytical Chemistry, Changchun Institute of Applied Chemistry, Chinese Academy of Sciences, Changchun 130022, PR China

[b] School of Applied Chemistry and Engineering, University of Science and Technology of China, Hefei, Anhui 230026, PR China

[c] Jilin Province Key Laboratory of Green Chemistry and Process, Changchun Institute of Applied Chemistry, Chinese Academy of Sciences, Changchun 130022, PR China

[d] Department of Chemistry, Northeast Normal University, Changchun 130024, PR China

[e] School of Environment, Northeast Normal University, Changchun 130117, PR China

*Corresponding author, Tel: +86-431-85262410; Fax: +86-431-85262410;

E-mail address: zhangc614@nenu.edu.cn, zhaofy@ciac.ac.cn

Number of pages: 21

Number of figures: 15

Number of tables: 7

Contents

Table S1. Physicochemical properties of Ru/SiO_2, $Ru/Ti\text{-}SiO_2$ and Ru/TiO_2 catalysts.

Catalyst	Volume of $TiCl_3$ solution introduced to 1.0 g of SiO_2 (mL)	BET surface area ($m^2 \cdot g^{-1}$)[a]	Average pore width (nm)	Ru particle size (nm)[b]	TiO_2 crystallite size (nm)[c]	Ti amount (wt %, Ti to SiO_2 mass ratio in 1 g support)[d]	Ti/Ru (theoretical molar ratio)	Surface Ti/ surface Si (atomic compositions)[e]
Ru/SiO_2	0	175	26.6	8.5	--	--	0	--
$Ru/3.3Ti\text{-}SiO_2$	0.5	154	32.2	7.7	--	3.3	2.3	--
$Ru/6.3Ti\text{-}SiO_2$	1	179	26.3	7.3	--	6.3	4.4	0.039
$Ru/15.6Ti\text{-}SiO_2$	3	157	16.4	5.4	--	15.6	11.0	--
$Ru/22.2Ti\text{-}SiO_2$	5	128	24.4	2.7	11.6	22.2	15.6	--
$Ru/27.1Ti\text{-}SiO_2$	7	114	20.4	2.5	11.1	27.1	19.1	0.089
$Ru/30.8Ti\text{-}SiO_2$	9	131	18.2	1.8	12.0	30.8	21.7	--
$Ru/33.8Ti\text{-}SiO_2$	11	143	16.6	1.8	11.7	33.8	23.8	--
$Ru/36.2Ti\text{-}SiO_2$	13	168	16.0	1.6	12.2	36.2	25.5	0.056
$Ru/42.0Ti\text{-}SiO_2$	20	72.7	20.2	1.0	13.2	42.0	29.6	0.075
Ru/TiO_2 (P25)	0	57.5	35.0	2.6	21.5	--	42.2	--
Ru/TiO_2 (rutile)	0	17.8	12.6	4.5	59.9	--	42.2	--

[a] Determined by nitrogen adsorption.

[b] Measured using CO pulse adsorption.

[c] Calculated using the Scherrer equation from XRD results, see Table S2.

[d] Obtained via: mass of Ti divided by mass of SiO_2. To obtain the mass of Ti derived from 1 mL of Ti-containing precursor, 1 mL of $TiCl_3$ aqueous solution (15-20 wt% in HCl) was dried at 80 °C and then calcined at 400 °C to form TiO_2 and finally weighed to calculate the mass of Ti.

[e] Estimated via XPS results.

Table S2. Results of TiO_2 crystallite sizes on reduced Ti-containing catalysts calculated using Scherrer equation.

Entry	Catalyst	2-Theta (°)	FWHM (°)	TiO_2 crystallite size (nm)
1	Ru/22.2TiSiO$_2$	27.36	0.70	11.6
2	Ru/27.1TiSiO$_2$	27.41	0.73	11.1
3	Ru/30.8TiSiO$_2$	27.36	0.67	12.0
4	Ru/33.8TiSiO$_2$	27.46	0.69	11.7
5	Ru/36.2TiSiO$_2$	27.41	0.66	12.2
6	Ru/42.0TiSiO$_2$	27.41	0.61	13.2
7	Ru/TiO$_2$ (P25)	25.30	0.37	21.5
8	Ru/TiO$_2$ (Rutile)	27.42	0.14	59.9

The crystallite sizes of TiO_2 in reduced Ru/Ti-SiO$_2$, Ru/TiO$_2$ (P25) and Ru/TiO$_2$ (Rutile) catalysts were estimated from the (110) diffraction signal of rutile (for Ti-modified catalysts and rutile-supported catalyst) and (101) diffraction signal of anatase (for P25 supported catalyst) using the Scherrer equation, $d = K\lambda/FWHM \cdot \cos\theta$, where λ is the wavelength of X-ray sources (for Cu Kα, λ = 1.54 Å), K = 0.89, θ is half of the diffraction angle and FWHM is the peak width at half of the maximum value of the diffraction peak. The structural parameters and the TiO_2 crystallite sizes calculated are shown in Table S1 above.

Table S3. Results for the hydrodeoxygenation of guaiacol at comparable conversion levels.

Entry	Catalyst	t (h)	Conv. (%)	Carbon balance (%)	Selectivity (%)		
					Phenol	Cyclohexanone	Cyclohexanol
1	Ru/SiO_2	24	17.7	88.9	78.3	10.4	11.3
2	$Ru/3.3TiSiO_2$	6	23.5	90.6	85.7	6.5	7.8
3	$Ru/6.3TiSiO_2$	3	14.6	94.5	81.8	8.2	10.0
4	$Ru/15.6TiSiO_2$	3	21.8	96.0	89.5	5.4	5.1
5	$Ru/27.1TiSiO_2$	1	15.1	95.8	82.5	7.3	10.2
6	$Ru/33.8TiSiO_2$	1	16.2	95.9	85.1	6.9	8.0
7	$Ru/36.2TiSiO_2$	1	18.9	96.2	85.3	8.1	6.6

Reaction conditions: 2 mmol guaiacol, 10 mL H_2O, 50 mg catalysts, 240 ºC, 0.4 MPa H_2.

Table S4. Influence of reduction temperature on the catalytic performance of Ru/Ti-SiO_2 and Ru/TiO_2 catalysts.

Entry	Catalyst	Reduction temperature (ºC)	Conv. (%)	Carbon balance (%)	Selectivity (%)			
					Phenol	Cyclohexanone	Cyclohexanol	Benzene
1	Ru/Ti-SiO_2	250	40.1	88.0	81.3	4.8	4.8	9.1
2		350	38.0	90.4	82.9	3.7	4.3	9.1
3		450	35.9	94.0	83.7	3.0	4.6	8.7
4		550	40.3	91.2	85.2	3.0	3.5	8.3
5	Ru/TiO_2	250	35.5	93.0	82.4	3.8	4.9	8.9
6		350	35.9	93.8	80.3	2.8	8.6	8.3
7		450	29.8	88.6	75.6	5.7	5.3	13.4
8		550	23.1	98.3	79.4	4.5	5.3	10.8

Reaction conditions: 2 mmol guaiacol, 10 mL H_2O, 50 mg catalyst, 240 ºC, 0.4 MPa H_2, 3 h.

Table S5. Influence of calcination temperature of Ti-SiO_2 support on the catalytic performance of Ru/Ti-SiO_2 catalyst.

Entry	Calcination temperature (ºC)	Conv. (%)	Carbon balance (%)	Selectivity (%)			
				Phenol	Cyclohexanone	Cyclohexanol	Benzene
1	400	39.2	88.5	83.6	4.2	4.1	8.1
2	600	37.1	94.8	82.3	4.7	4.2	8.8
3	800	22.5	90.7	86.9	6.6	6.5	--

Reaction conditions: 2 mmol guaiacol, 10 mL H_2O, 50 mg catalyst, 240 ºC, 0.4 MPa H_2, 3 h.

Table S6. Results of TiO_2 crystallite sizes on Ru/Ti-SiO_2 catalysts with support treated at different temperatures, as estimated according to Scherrer equation.

Entry	Catalyst	2-Theta (º)	FWHM (º)	TiO_2 crystallite size (nm)
1	Ru/Ti-SiO_2-400	27.41	0.730	11.1
2	Ru/Ti-SiO_2-600	27.45	0.560	14.4
3	Ru/Ti-SiO_2-800	27.41	0.337	24.0

Table S7. HDO of guaiacol with various heterogeneous catalysts.

Entry	Catalyst	Reactor	T(°C)	P(bar)	Solvent	Conv. (%)	Product/ Sele. (%)	Ref.
1	Unsupported Mo_2N-A	batch	300	50	decalin	95	phenol/~90	1
2	(Mo_2C@C)	batch	340	28	methanol	76	phenol/69	2
3	W_2C/CNF	batch	375	55	dodecane	>99	phenol/~70	3
4	Mo_2C/CNF	batch	375	55	dodecane	>99	phenol/~50	3
5	Mo/C	fixed-bed	400	40	--	98	phenol/76.5	4
6	Au/TiO_2	batch	300	65	toluene	~43	phenol/~59	5
7	Ag/TiO_2	batch	300	30	heptane	~75	phenol/ ~59	6
8	Ni/TiO_2	batch	300	40	decane	~99	phenol/ ~83	7
9	NiFe/CNF	fixed-bed	300	30	--	47	phenol/83	8
10	Au/TiO_2	fixed-bed	280	40	--	~57	phenol/~82	9
11	Fe/CeO_2	fixed-bed	400	1	--	phenol yield: 56%		10
12	PtFe/CeO_2	fixed-bed	400	1	--	phenol yield: 57%		11
13	Pt/WC	fixed-bed	300	30	--	78.6	phenol/89.0	12
14	α-MoSn	batch	300	40	n-hexane	100	phenol/92.5	13
15	Ru/Cl/TiO_2	batch	240	4	1,4-dioxane	~64	phenol/~40	14
16	Ru/Ti-SiO_2	batch	240	4	H_2O	83.6	phenol/70.4 benzene/10.6	This work

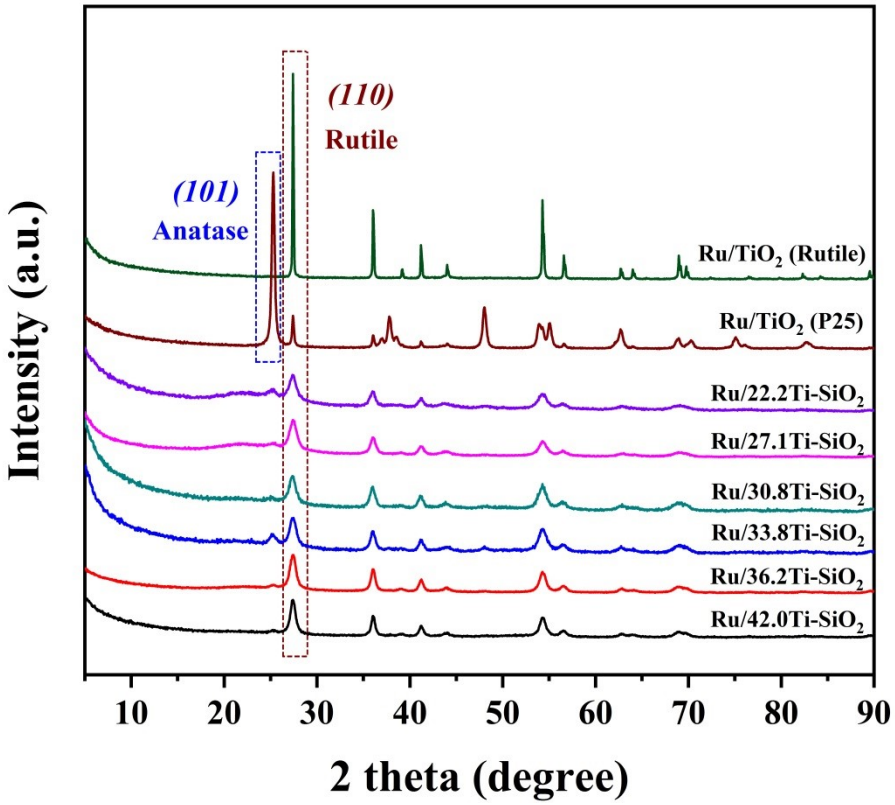

Fig. S1. XRD patterns of Ru/Ti-SiO_2, Ru/TiO_2 (P25) and Ru/TiO_2 (Rutile) catalysts.

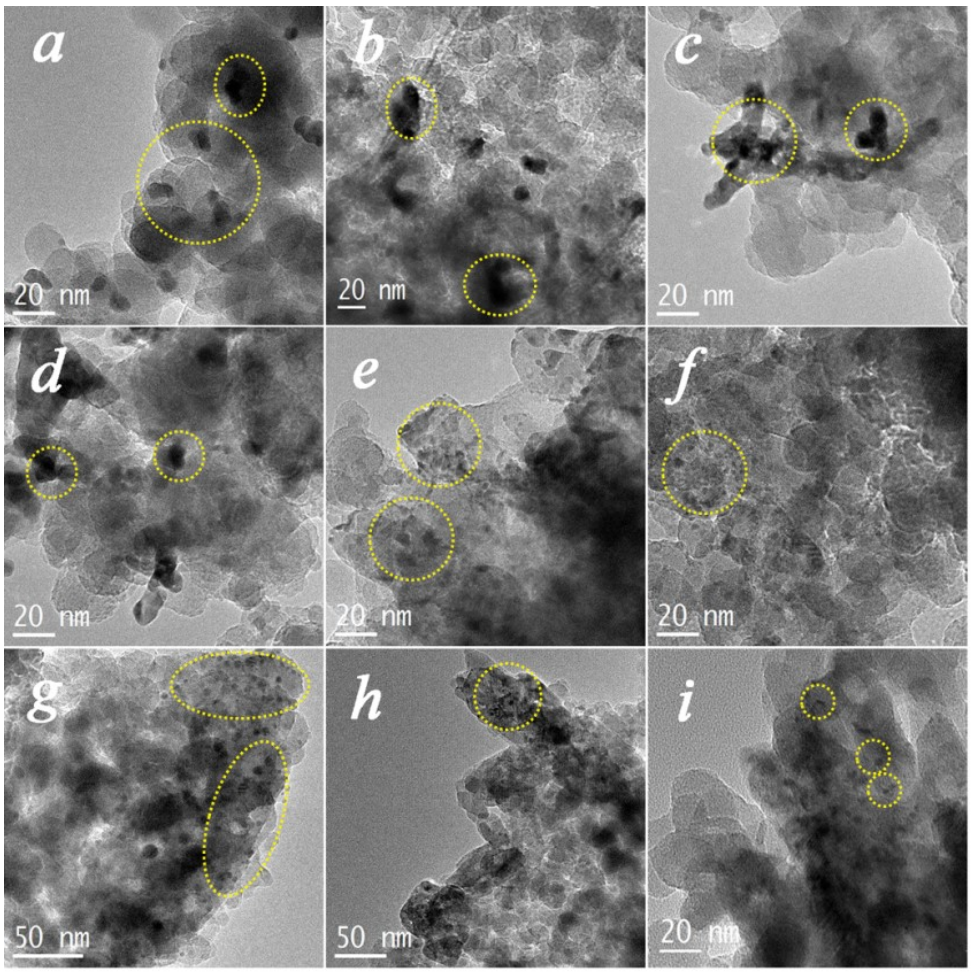

Fig. S2. TEM images of Ru/SiO_2 and Ru/Ti-SiO_2 catalysts. (a) Ru/SiO_2, (b) Ru/3.3Ti-SiO_2, (c) Ru/6.3Ti-SiO_2, (d) Ru/15.6Ti-SiO_2, (e) Ru/22.2Ti-SiO_2, (f) Ru/27.1Ti-SiO_2, (g) Ru/30.8Ti-SiO_2, (h) Ru/33.8Ti-SiO_2, (i) Ru/42.0Ti-SiO_2. The yellow dotted line highlights Ru particles.

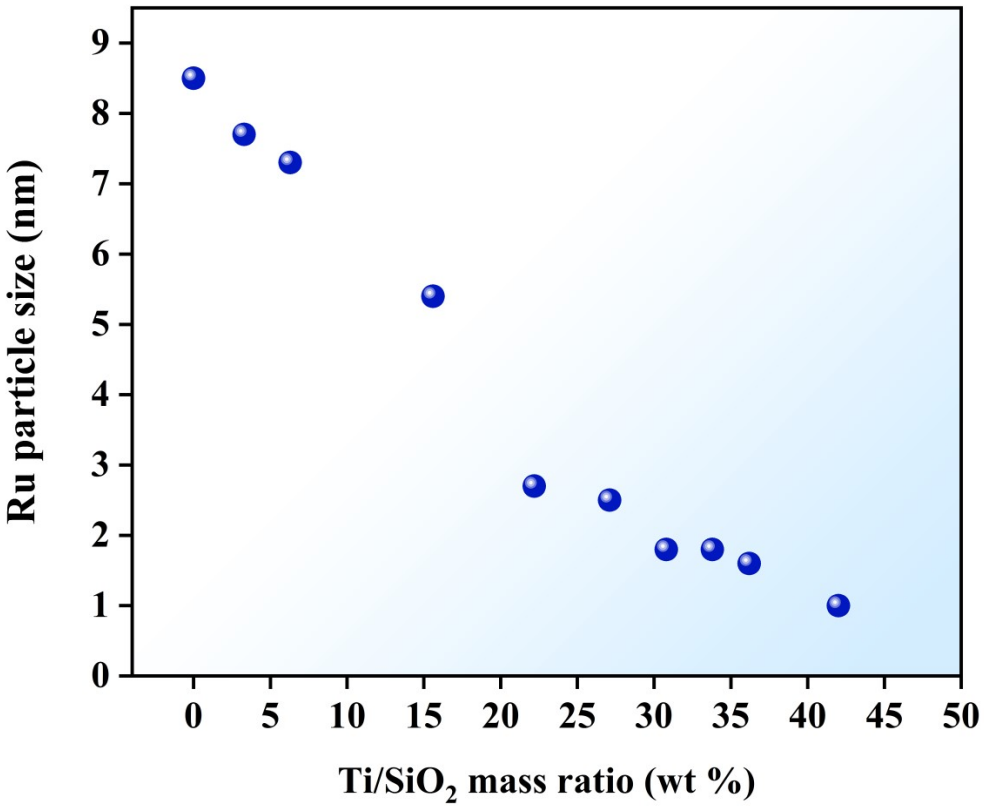

Fig. S3. The relationship between Ru particle size and Ti amount in Ru/Ti-SiO_2 catalysts.

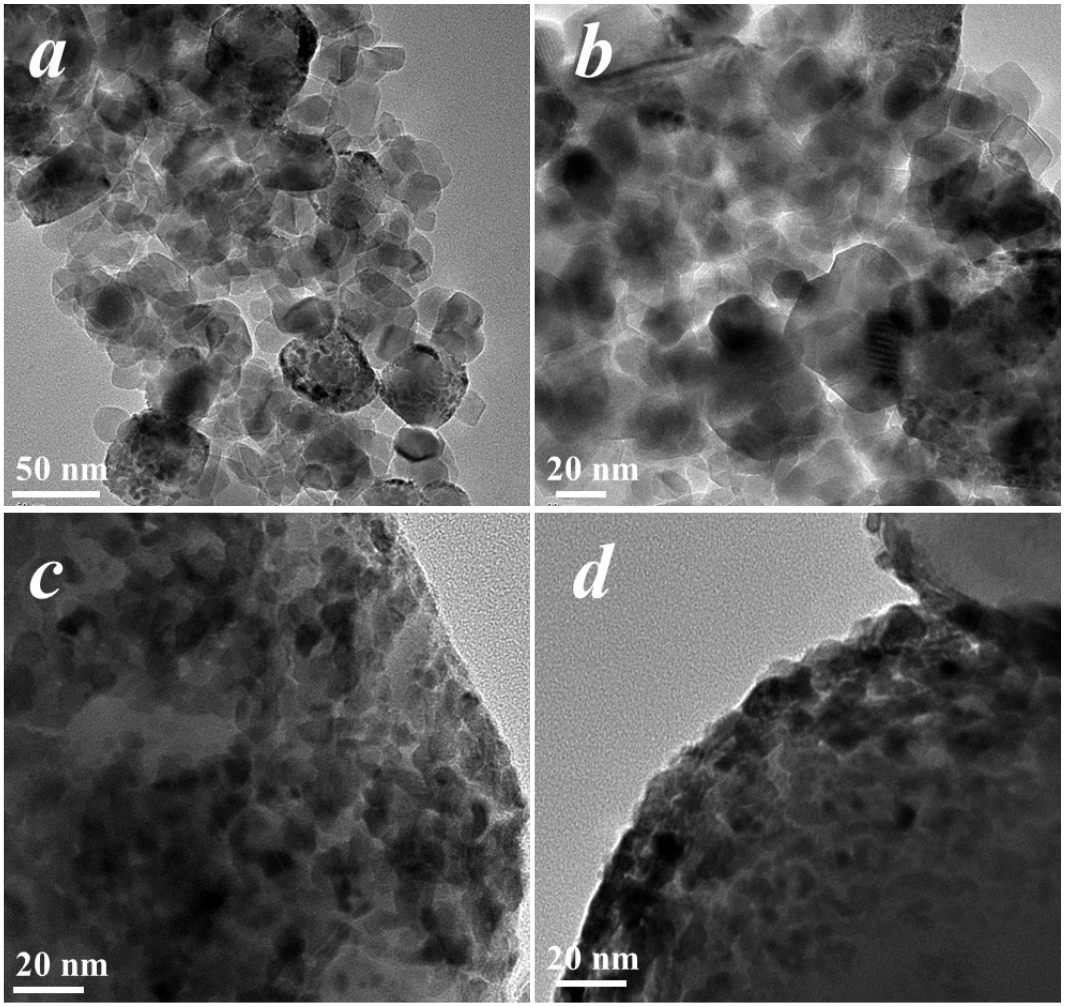

Fig. S4. TEM images of Ru/TiO_2 catalysts. (a-b) Ru/TiO_2-P25; (c-d) Ru/TiO_2-rutile.

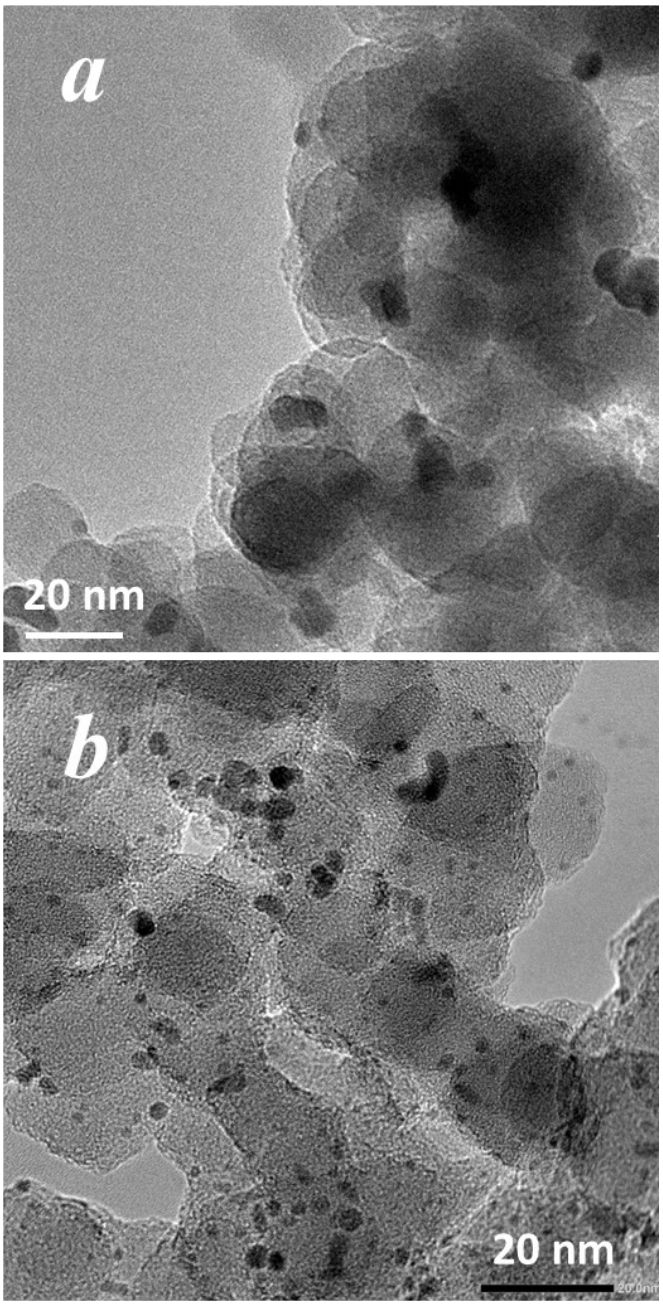

Fig. S5. TEM images of (a) Ru/SiO_2-A and (b) Ru/SiO_2-B.

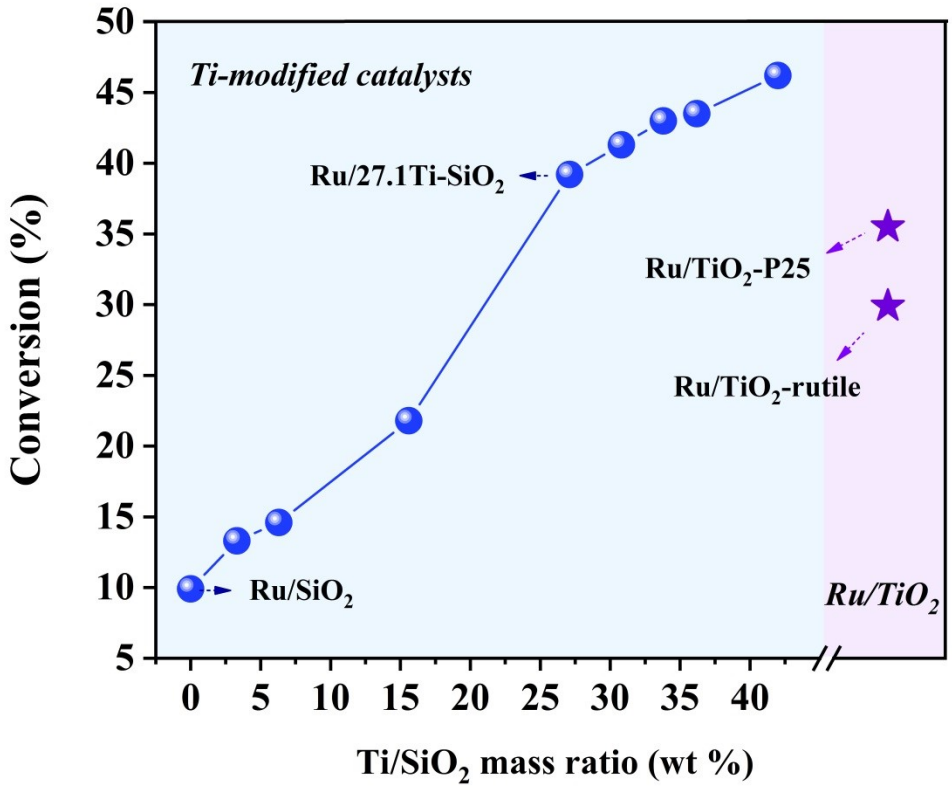

Fig. S6. Catalytic performance of Ru/SiO_2, Ru/TiO_2 and $Ru/Ti\text{-}SiO_2$ catalysts. Light blue area stands for $Ru/Ti\text{-}SiO_2$ catalysts and light pink area for Ru/TiO_2 catalysts.

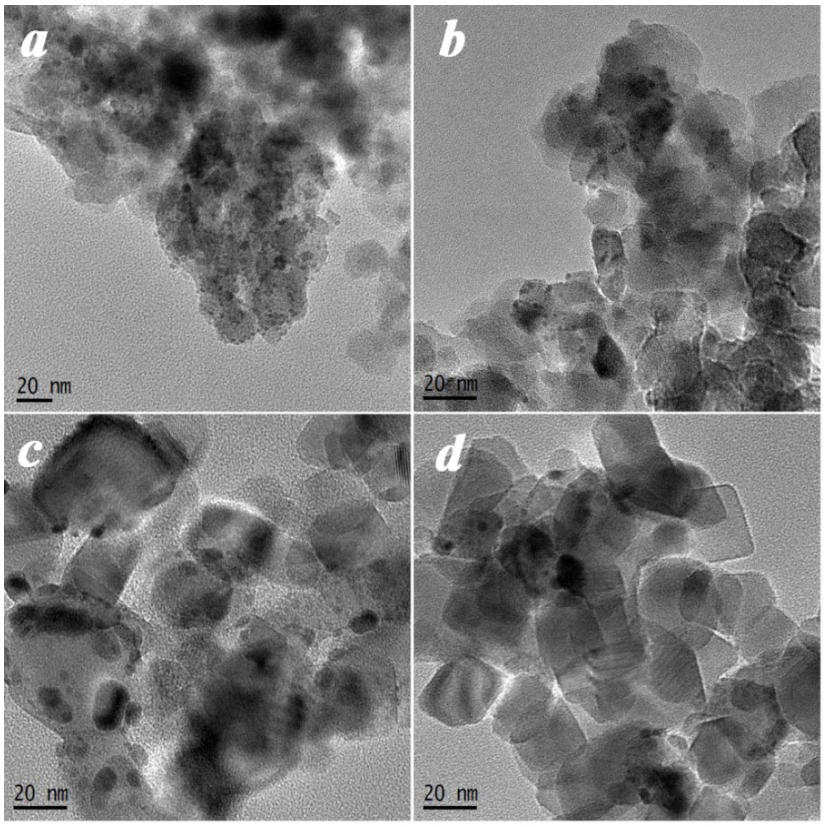

Fig. S7. TEM images of (a-b) Ru/Ti-SiO_2 and (c-d) Ru/TiO_2 (P25) catalysts reduced at 550 ºC.

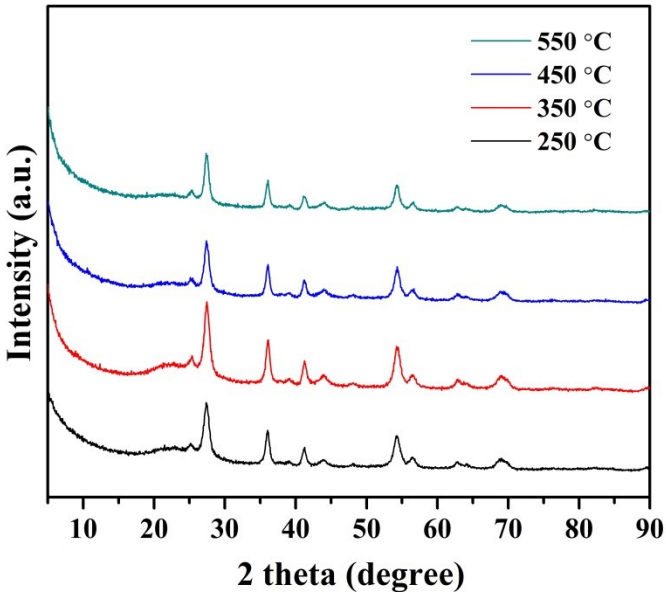

Fig. S8. XRD patterns of Ru/Ti-SiO_2 catalyst reduced at different temperatures.

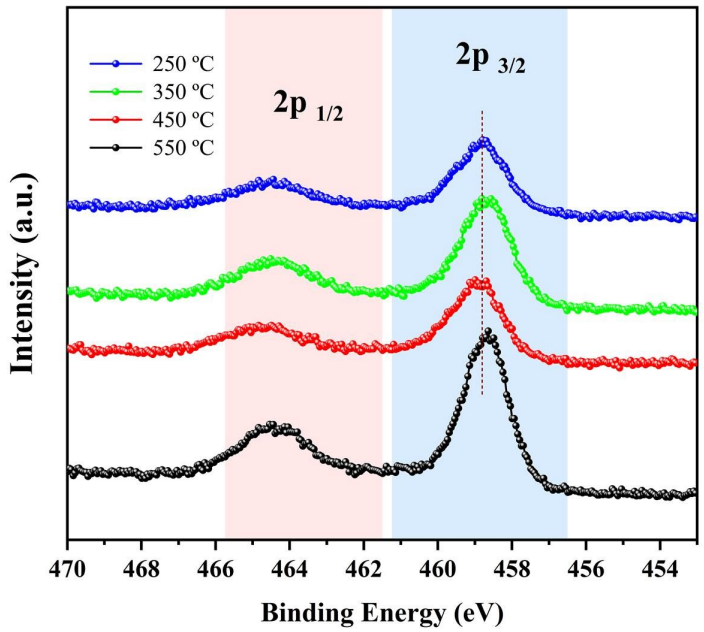

Fig. S9. Ti 2p XPS spectra of Ru/Ti-SiO_2 catalysts reduced at different temperatures.

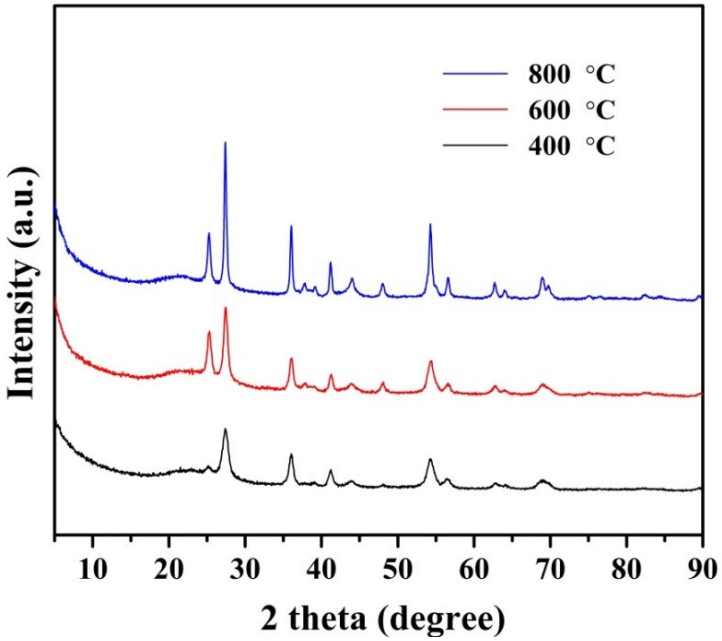

Fig. S10. XRD patterns of Ru/Ti-SiO_2 catalysts in which Ti-SiO_2 support was calcined at different temperatures in static air for 3 h.

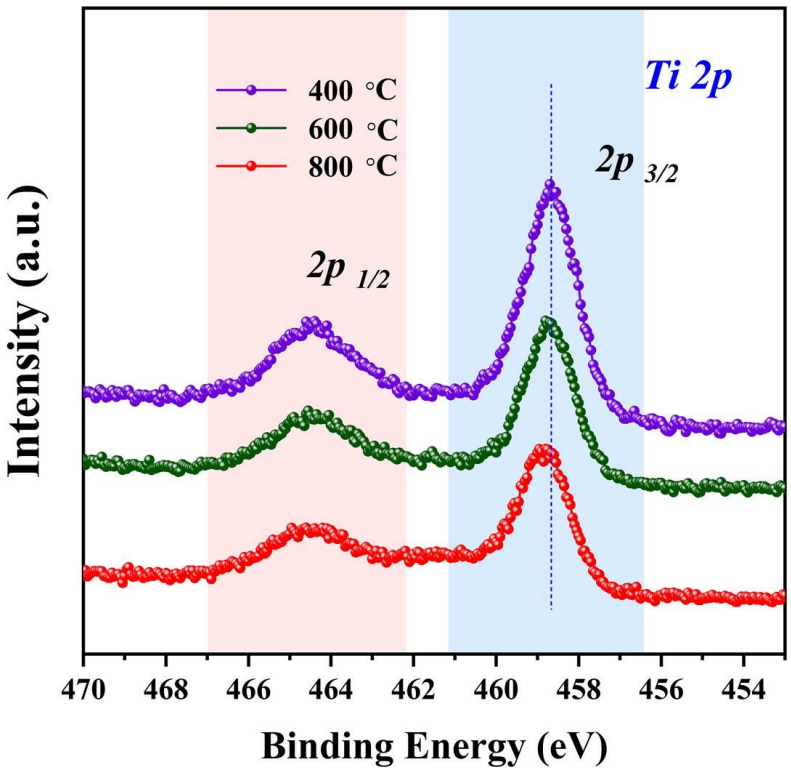

Fig. S11. Ti 2p XPS spectra of Ru/Ti-SiO_2 catalysts in which Ti-SiO_2 support was calcined at different temperatures in static air for 3 h.

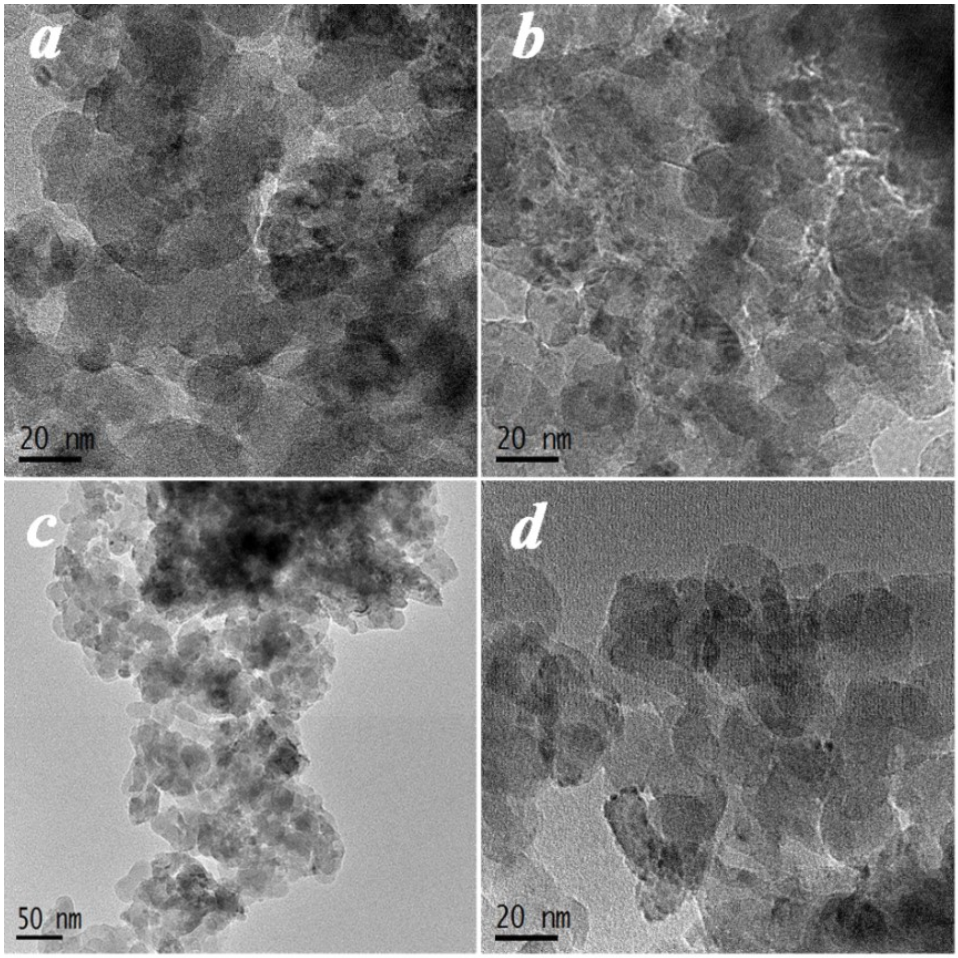

Fig. S12. TEM images of Ru/Ti-SiO_2 catalysts with different Ru loadings. (a) 1 wt % Ru, (b) 3 wt % Ru, (c) 6 wt % Ru and (d) 9 wt % Ru.

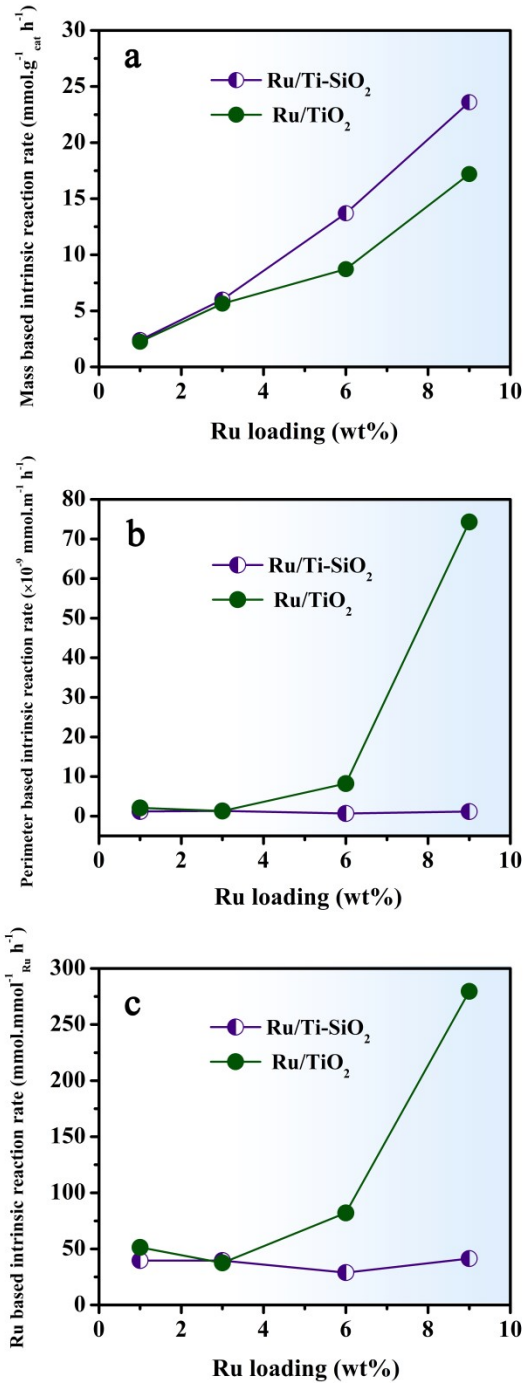

Fig. S13. Effect of Ru loading on intrinsic reaction rates of guaiacol conversion on Ru/Ti-SiO_2 and Ru/TiO_2 (P25) catalysts based on (a) mass of catalyst, (b) perimeter of Ru and (c) amount of surface Ru. Reaction conditions: 2 mmol guaiacol, 10 mL H_2O, 240 ºC, 0.4 MPa H_2, 1 h, guaiacol:Ru = 135:1 (mol/mol).

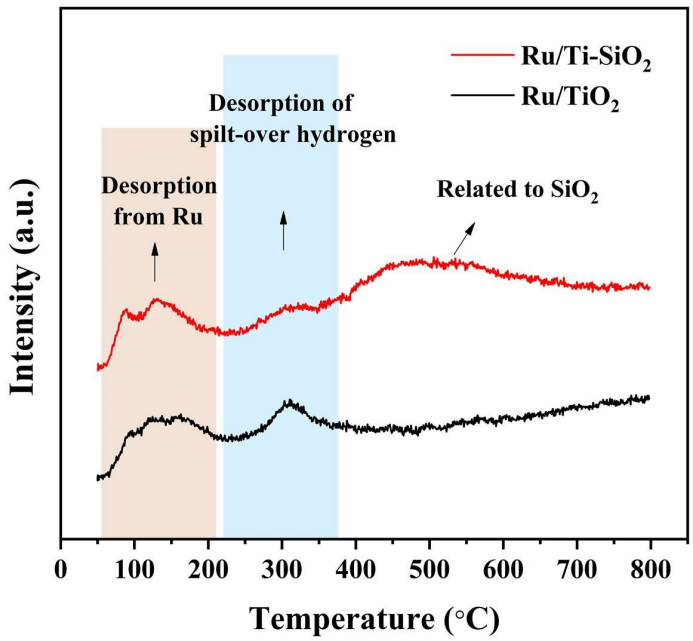

Fig. S14. H_2-TPD profiles of Ru/Ti-SiO_2 and Ru/TiO_2 catalysts.

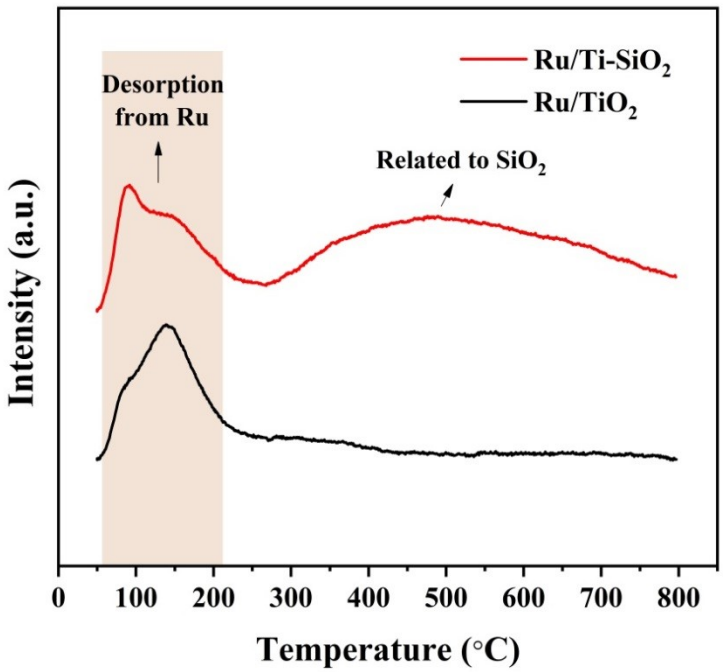

Fig. S15. CO-TPD profiles of Ru/Ti-SiO_2 and Ru/TiO_2 catalysts.

Notes and references

1. I. T. Ghampson, C. Sepúlveda, R. Garcia, B. G. Frederick, M. C. Wheeler, N. Escalona and W. J. DeSisto, *Appl. Catal. A*, **2012**, 413-414, 78-84.
2. R. Li, A. Shahbazi, L. Wang, B. Zhang, A. M. Hung and D. C. Dayton, *Appl. Catal. A*, **2016**, 528, 123-130.
3. A. L. Jongerius, R. W. Gosselink, J. Dijkstra, J. H. Bitter, P. C. A. Bruijnincx and B. M. Weckhuysen, *ChemCatChem*, **2013**, 5, 2964-2972.
4. J. Chang, T. Danuthai, S. Dewiyanti, C. Wang and A. Borgna, *ChemCatChem*, **2013**, 5, 3041-3049.
5. J. Mao, J. Zhou, Z. Xia, Z. Wang, Z. Xu, W. Xu, P. Yan, K. Liu, X. Guo and Z. C. Zhang, *ACS Catal.*, **2016**, 7, 695-705.
6. K. Liu, P. Yan, H. Jiang, Z. Xia, Z. Xu, S. Bai and Z. C. Zhang, *J. Catal.*, **2019**, 369, 396-404.
7. X. Zhang, P. Yan, B. Zhao, K. Liu, M. C. Kung, H. H. Kung, S. Chen and Z. C. Zhang, *ACS Catal.*, **2019**, 9, 3551-3563.
8. H. Fang, J. Zheng, X. Luo, J. Du, A. Roldan, S. Leoni and Y. Yuan, *Appl. Catal. A*, **2017**, 529, 20-31.
9. T.-S. Nguyen, D. Laurenti, P. Afanasiev, Z. Konuspayeva and L. Piccolo, *J. Catal.*, **2016**, 344, 136-140.
10. C. Li, Y. Nakagawa, M. Tamura, A. Nakayama, K. Tomishige, *ACS Catal.*, **2020**, 10, 14624-14639.
11. C. Li, Y. Nakagawa, M. Yabushita, A. Nakayama, K. Tomishige, *ACS Catal.*, **2021**, 11, 12794-12814.
12. H. Fang, L. Wu, W. Chen, Y. Yuan, *Appl. Catal. A.*, **2021**, 613, 118023.
13. X. Diao, N. Ji, T. Li, Z. Jia, S. Jiang, Z. Wang, C. Song, C. Liu, X. Lu, Q. Liu, *J. Catal.*, **2021**, 401, 234-251.
14. X. Wang, P. Wu, Z. Wang, L. Zhou, Y. Liu, H. Cheng, M. Arai, C. Zhang, F. Zhao, *ACS Sustainable. Chem. Eng.*, **2021**, 9, 3083-3094.